nature genetics

A module of negative feedback regulators defines growth factor signaling

Ido Amit[1,9], Ami Citri[1,8,9], Tal Shay[2], Yiling Lu[3], Menachem Katz[1], Fan Zhang[3], Gabi Tarcic[1], Doris Siwak[3], John Lahad[3], Jasmine Jacob-Hirsch[4], Ninette Amariglio[4], Nora Vaisman[5], Eran Segal[6], Gideon Rechavi[4], Uri Alon[7], Gordon B Mills[3], Eytan Domany[2] & Yosef Yarden[1]

Signaling pathways invoke interplays between forward signaling and feedback to drive robust cellular response. In this study, we address the dynamics of growth factor signaling through profiling of protein phosphorylation and gene expression, demonstrating the presence of a kinetically defined cluster of delayed early genes that function to attenuate the early events of growth factor signaling. Using epidermal growth factor receptor signaling as the major model system and concentrating on regulation of transcription and mRNA stability, we demonstrate that a number of genes within the delayed early gene cluster function as feedback regulators of immediate early genes. Consistent with their role in negative regulation of cell signaling, genes within this cluster are downregulated in diverse tumor types, in correlation with clinical outcome. More generally, our study proposes a mechanistic description of the cellular response to growth factors by defining architectural motifs that underlie the function of signaling networks.

Cells respond in a stereotypic and highly reproducible manner to external stimuli. A major focus of current research is elucidation of the mechanisms underlying the regulation of this response. In the past, considerable effort was invested in characterizing 'forward-signaling' components activated by external stimuli, with successful identification of proteins involved in signaling cascades and immediate-early genes encoding transcription factors. However, in recent years, the focus of the signal transduction field has shifted to identification of feedback regulatory components. The clinical rationale is obvious: the function of these components, which define the specificity and extent of growth factor signaling, is often imbalanced during oncogenic transformation[1]. Although an increasing number of such gene products have been identified, an overall understanding of feedback control within signal transduction systems has not been achieved. The recent advent of systems biology suggests a potential strategy for deciphering organizational principles of signaling networks by analyzing the dynamics of network components, which we will exploit in this study[2–4].

The epidermal growth factor (EGF) ErbB system is one of the best studied signaling networks[4]. Disregulated activation of this network has been implicated in diverse types of human cancer, primarily in carcinomas of secretory epithelia[5]. Here we address the dynamics of signal transduction events induced by EGF at the level of phosphorylation and gene expression, with the aim of uncovering mechanisms of transcription-dependent signal attenuation. Consequently, we can now identify a cluster of coexpressed genes that function in feedback attenuation of growth factor signaling at specific nodes within the network (for an overview, see **Supplementary Fig. 1** online). In the case of EGF, a central feedback node is at the tier of mitogen-activated protein kinases (MAPKs) and is attenuated through induction of specific phosphatases. Downstream, transcription regulators and RNA-binding proteins further attenuate the initial burst of transcription. The induction of negative regulators therefore serves to attenuate the same pathway that induced their expression, leading to the definition of an activation interval. The assembly of these components into network motifs suggests organizational principles coordinating robust growth factor signaling. Notably, the identities of the active components vary between systems, but the overall signaling architecture is conserved across cell types and stimuli.

Transcription-dependent attenuation of EGF signaling

The cellular response to EGF is initiated by rapid kinetics of receptor activation, followed by phosphorylation-dependent activation of signaling cascades. This is typically analyzed by observing activation of the ERK MAPKs and subsequent transcriptional activation of immediate-early genes (IEGs) such as the AP-1 components *FOS*

[1]Department of Biological Regulation and [2]Department of Physics of Complex Systems, The Weizmann Institute of Science, Rehovot 76100, Israel. [3]Department of Systems Biology, MD Anderson Cancer Center, Houston, Texas 77030, USA. [4]Department of Pediatric Hemato-Oncology and Functional Genomics, The Chaim Sheba Medical Center and Sackler School of Medicine, Tel Aviv University, Tel Aviv 69978, Israel. [5]Sigma-Aldrich Israel, Ltd., Rehovot 76100, Israel. [6]Department of Computer Science and [7]Department of Molecular Cell Biology, The Weizmann Institute of Science, Rehovot 76100, Israel. [8]Current address: Department of Psychiatry and Behavioral Sciences, Stanford University Medical School, Palo Alto, California 94304-5485, USA. [9]These authors contributed equally to this work. Correspondence should be addressed to Y.Y. (yosef.yarden@weizmann.ac.il).

Received 13 September 2006; accepted 24 January 2007; published online 25 February 2007; doi:10.1038/ng1987

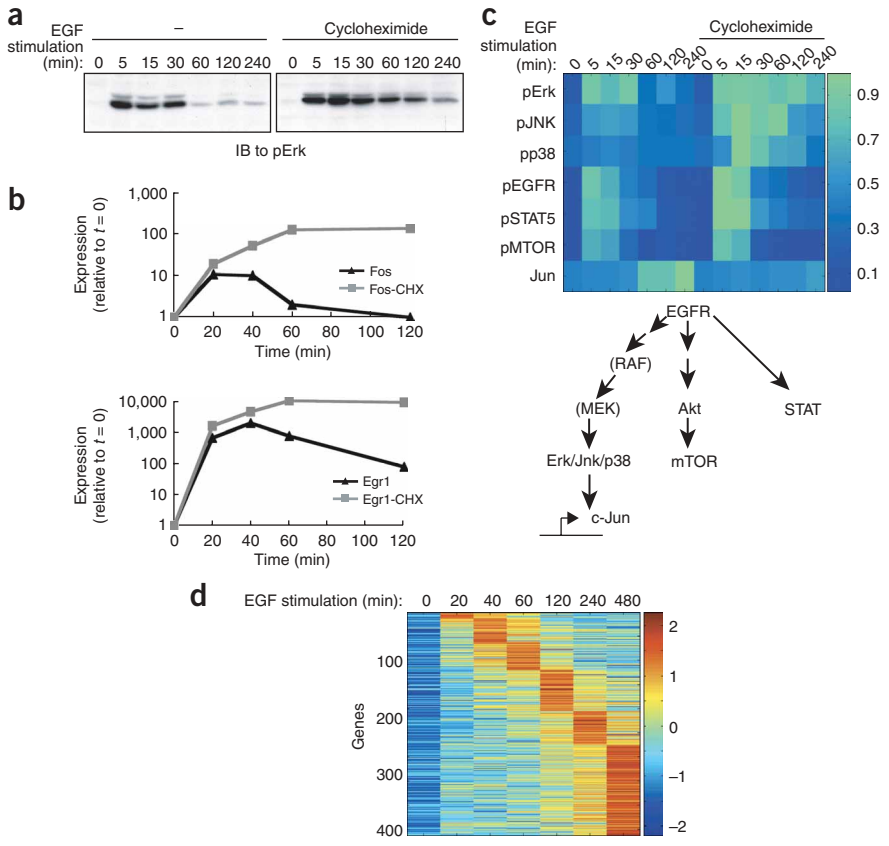

Figure 1 MAPKs are a node of transcription-dependent feedback regulation. (**a**) Subconfluent HeLa cells were serum starved for 24 h and then stimulated with EGF (20 ng/ml) for the indicated time intervals in the absence or presence of cycloheximide (1 μg/ml). ERK activation was assayed by immunoblotting (IB) of cell extracts with antibodies to the active form of ERK. (**b**) HeLa cells, plated and starved as in **a,** were subjected to stimulation with EGF, with or without a pretreatment with cycloheximide (CHX) for 10 min. Total RNA prepared from cell lysates was subjected to reverse transcription with random hexamers and analysis by quantitative real-time PCR with primers specific to *FOS* and *EGR1*. The signals were quantified (relative to time zero). (**c**) Subconfluent HeLa cells were serum starved for 24 h and then stimulated with EGF (20 ng/ml) for the indicated time intervals in the absence or presence of cycloheximide (1 μg/ml), and cell extracts were analyzed by quantitative reverse-phase protein lysate arrays (**Supplementary Methods** and **Supplementary Table 1**). Data are presented as fraction of peak response. The chart underneath schematically presents the pathways analyzed using antibodies to phosphorylated forms of the indicated proteins. (**d**) Serum-starved HeLa cells were stimulated with EGF for the indicated time intervals, followed by analysis of RNA expression using Affymetrix Hu-133A oligonucleotide microarrays (containing ~22,000 human probe sets). The 465 genes whose expression was induced to at least twice the baseline level were ordered according to their peak expression time.

and *JUN* or the zinc finger transcription factor *EGR1* (ref. 6). To assess the role of transcription in attenuation of EGF signaling, we treated HeLa cells (a common model system for investigation of growth factor signaling) with EGF in the presence or absence of the protein translation inhibitor cycloheximide. We observed that attenuation of ERK signaling (**Fig. 1a**), as well as attenuation of immediate-early transcription (**Fig. 1b**), is dependent on *de novo* gene transcription. This demonstrates a central role for transcription-mediated feedback control in defining the interval of downstream phosphorylation and transcriptional events, a finding consistent with previous observations[7,8].

MAPKs constitute a node of feedback regulation

In order to define the nodes of EGF-activated phosphorylation cascades subject to feedback regulation, we used the emerging technology of reverse-phase protein lysate arrays (RPPA; **Fig. 1c** and **Supplementary Table 1** online). This assay has been calibrated extensively to ensure specificity and quantitative reliability in analysis of a large number of samples across a variety of antibodies[9] (see **Supplementary Methods** online for explanation of the methodology and description of the antibodies used). We used 32 different antibodies, 19 of which addressed the phosphorylation state of 16 proteins within the pathway.

The results demonstrate that the ERK and STAT5 cascades are those most robustly activated by EGF in HeLa cells. In the presence of the translational inhibitor cycloheximide (or the transcriptional inhibitor actinomycin D; data not shown), the activation interval of the MAPK tier (ERK, JNK and p38) was markedly prolonged. Notably, we did not observe any obvious effects on the kinetics of other tiers within the same cascade, nor did we find any effect on other signaling cascades (**Fig. 1c** and **Supplementary Table 1**). Thus, transcription-dependent attenuation acts at specific nodes within signal transduction cascades, with the MAPK tier being the major target of this mechanism within EGF-activated cascades.

Notably, proteins previously characterized as EGF-induced negative-feedback regulators, such as Sprouty-2 and Mig-6 (ref. 10), have been demonstrated to repress the activity of the EGF receptor or other proteins at a similarly high level in the signaling hierarchy. As the peak induction of these proteins occurs 60–120 min after stimulation (data not shown), they are active only after the EGF receptor has been degraded, suggesting that they do not function as feedback regulators of signaling. Rather, we are led to assume that these proteins maintain a 'refractory period' that decouples the cell from repetitive stimulation (ref. 11 and data not shown). Recent observations concerning the function of Sprouty proteins in tooth development are congruent with this hypothesis[12].

The circuitry of growth factor–induced transcription

As we aimed to identify the mechanisms of transcription-dependent feedback attenuation of growth factor signaling, we constructed a comprehensive kinetic profile of the transcriptional response of HeLa cells to EGF (**Fig. 1d** and **Supplementary Table 1**). We were surprised at the coherence of the resulting expression matrix, which showed clearly defined waves of transcription. The initial wave demonstrated rapid induction of a small number of previously characterized IEGs at the first time point (20 min; 14 genes). Examining the identity of genes within subsequent waves of transcription, we realized that the coordinate expression could be strongly correlated with similarity of

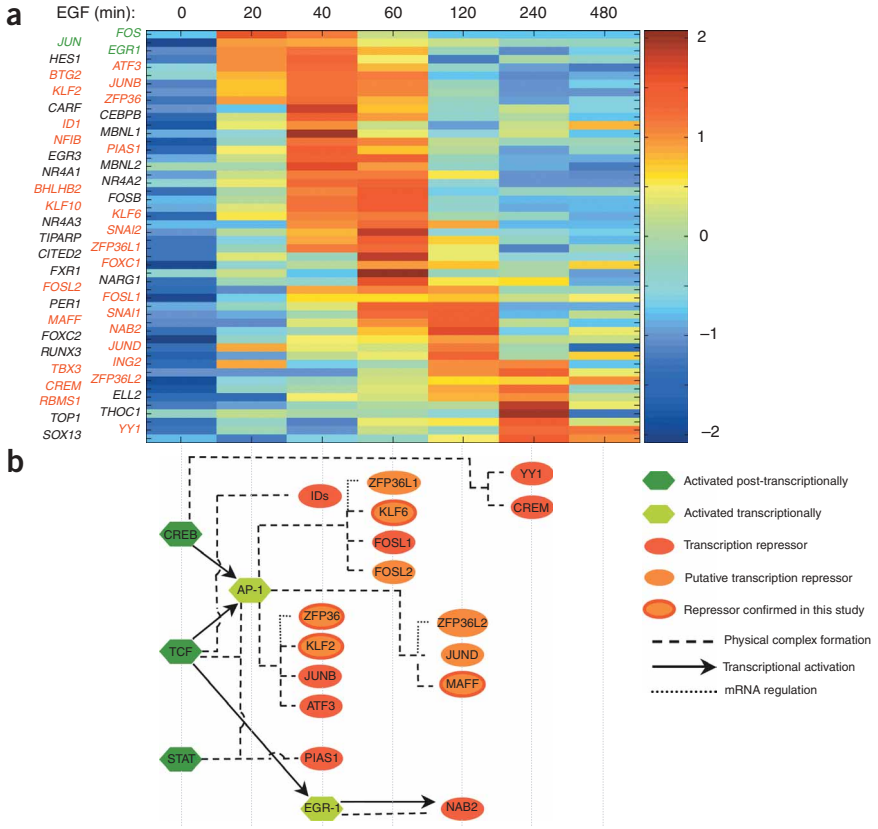

Figure 2 Circuitry of growth factor–induced transcriptional regulation. (**a**) Expression matrix of transcripts induced by EGF in HeLa cells. Shown are transcripts that encode nucleotide-binding proteins, according to the Gene Ontology database. Genes were ordered according to their peak expression time. Gene symbols are color coded according to their reported predominant function in signaling networks (green, transcription activators; red, transcription repressors). (**b**) Interaction map of proteins implicated as participating in the EGF-induced transcriptional program. The genes are organized according to their peak induction time (note alignment with the expression matrix shown in **a**).

protein function. This observation is in line with the concept that coordinately expressed genes often share similar cellular function[13–16]. Obvious candidate proteins responsible for the attenuation of MAPK signaling are the MAPK phosphatases (MKPs, or dual-specificity phosphatases), a number of which have been reported to undergo transcriptional induction after growth factor activation[17]. Indeed, we observed coordinate induction of multiple dual-specificity phosphatases in EGF-treated HeLa cells (see below).

To identify potential feedback regulators responsible for the attenuation of EGF-driven transcription, we examined the subset of genes whose transcription peaked between 20 and 240 min after stimulation and that are classified as nucleotide-binding according to the Gene Ontology database (**Fig. 2a**; see URLs in Methods section). This set of 50 genes contained mainly transcriptional regulators and RNA-binding proteins. The classic IEGs, *FOS*, *JUN* and *EGR1*, which are 'forward-driving' transcription factors (peaking at 20–40 min), belong to a relatively small subset, whereas a large fraction (25/47) of the genes induced at later time points (peaking at 40–240 min (hereafter referred to as delayed early genes or DEGs)) have been implicated in negative transcriptional regulation (for functional annotation and references, see **Supplementary Table 1**). The theme of coordinated expression and function alluded to in previous publications[15,16] can be extended to the cluster of coexpressed nucleotide-binding proteins. Adopting this theme as a guide for annotating gene function, we propose a negative regulatory function for the noncharacterized gene products found within the cluster of DEGs.

With that in mind, we searched for examples of delayed induction of a transcriptional attenuator and found several cases. In many instances, the transcriptional attenuator forms a physical complex with and attenuates the function of a transcriptional activator that is induced earlier: for example, NAB2 binds and inhibits active complexes of EGR1 (ref. 18); FOSL1 binds with and inhibits active AP-1 complexes[19]; JUNB engages AP-1 complexes and inhibits activation of JUN[20] and ID2 is induced in a delayed fashion to inhibit the activation of the TCF complex[21]. Finally, ATF3 is induced in a delayed fashion and binds elements found in proximity to AP-1 and NFκB elements, repressing gene transcription by these two transcription activators[22]. Extending these observations to a wider group of transcription regulators, we constructed a network map describing the nodes, 'transcriptional edges' and previously documented physical interactions within this set (see URLs for the Human Protein Reference Database in Methods and **Supplementary Table 1**), as well as relationships with phosphoregulated transcription factors reported to be activated by EGF (STAT, CREB and TCF). We displayed the connectivity against the time of peak induction (**Fig. 2b**) for both previously known feedback regulators as well as those that we identified and confirmed for the first time in this work. This network map suggests a coordinated, time-dependent change in the composition of transcriptional complexes after recruitment of newly synthesized DEGs. We propose that the recruitment of these regulators into existing transcriptional complexes results in attenuation of their transcriptional activity. These kinetics would permit transient activation of specific transcription complexes, followed by rapid attenuation, consistent with the observed waves of EGF-induced transcription (**Fig. 1d**). These waves of transcription are specifically demonstrated by the peak induction (60–120 min) of a cluster of ligands and cytokines, a common physiological measure of growth factor–driven response (output) regulated by AP-1 activity[23,24] (**Supplementary Fig. 2** online).

KLF2 and MAFF are feedback regulators

To verify the regulatory function of potential novel transcriptional repressors within the DEG cluster, we focused on three molecules (**Fig. 3a**): the Kruppel-like factors 2 and 6 (KLF2 and KLF6) and avian musculoaponeurotic fibrosarcoma oncogene family, protein F (MAFF). The KLFs are SP1-like transcription factors[25], and MAFF is a small MAF family protein, lacking the transactivation domain[26] characteristic of active transcription factors (similar to the transcriptional repressor FOSL1 (ref. 27)). We verified EGF-mediated

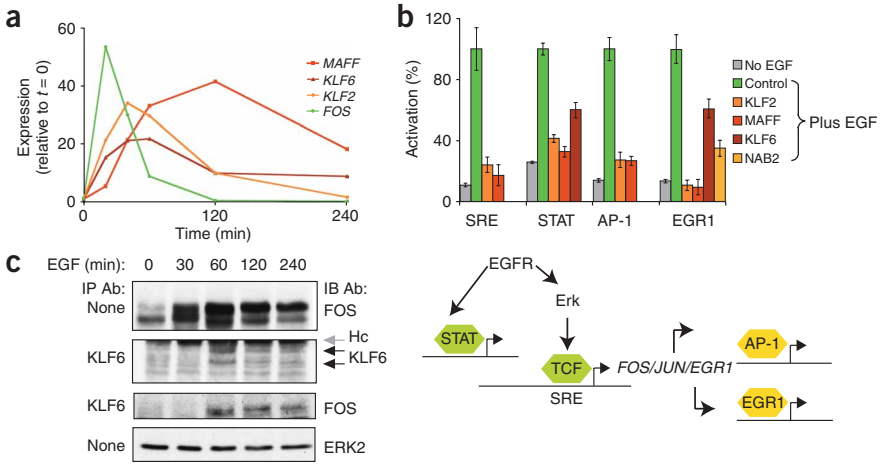

Figure 3 The delayed early genes *MAFF*, *KLF2* and *KLF6* repress EGF-driven gene transcription. (**a**) EGF-induced expression of *KLF6*, *KLF2* and *MAFF*, in comparison with *FOS* (derived from the HeLa transcriptional data set). (**b**) HeLa cells were cotransfected with 100 ng plasmids encoding GFP (*con*), GFP-MAFF, GFP-KLF2, GFP-KLF6 or NAB2, along with the indicated luciferase reporter plasmid, as illustrated in the schematic below the graph. Twenty-four hours after transfection, cells were serum starved for 16 h and stimulated with EGF for 4 h, and then luminescence was determined. The results are presented as a percentage of the maximal signal (green bars) ± s.d. of three replicates. (**c**) Serum-starved HeLa cells were treated with EGF for the indicated time intervals, and extracts were subjected to immunoprecipitation (IP) of Klf6, followed by immunoblotting (IB) as indicated. Note the doublet of KLF6 (arrows) and the heavy chain of immunoglobulins (Hc).

apparent on TNFα-driven NFκB transcriptional activity (**Supplementary Fig. 3**). Consistent with recent observations[28], these results demonstrate the potential relevance of our observations to other signaling pathways. Notably, when testing the effects of KLF2 and MAFF on EGF-induced SP1 activity, we observed repression of SP1 activity by MAFF but activation of SP1 by KLF2 (**Supplementary Fig. 3**). As we discuss below, this may illustrate the time- and context-dependent flexibility of transcriptional modulators, which act as repressors in some contexts and activators in others. Numerous analogous examples are available in the literature; even the classic transcriptional activator FOS has been found to repress transcription in some contexts[29], and the transcriptional repressors NAB2 (ref. 30), ATF[31] and JUND[32] have been found to promote context-dependent transcriptional activation. We postulate time-dependent incorporation of the newly expressed DEGs into transcriptional complexes, and, as expected, we observed a physical association of the EGF-induced KLF6 protein with the FOS complex (**Fig. 3c**).

expression of these genes by quantitative PCR (data not shown) and confirmed the induction of MAFF and KLF6 gene products in different epithelial cell lines by immunoblotting (**Supplementary Fig. 3** online and data not shown). Ectopic expression of the cloned cDNAs at levels comparable to those attained upon stimulation with EGF resulted in inhibition of EGF-driven transcription through SRE- and STAT-responsive promoter elements as well as inhibition of the transcriptional activity of EGR1 and AP-1, which are encoded by IEGs (**Fig. 3b**; for additional evidence, see **Supplementary Fig. 3**). The inhibitory activity of MAFF and KLF2 was also

ZFP36 regulates stability of EGF-induced mRNA molecules

Early work[8] suggested that the superinduction of IEGs observed upon stimulation of cells in the presence of protein synthesis inhibitors occurs through disruption of two complementary processes: attenuation of transcription and induction of mRNA degradation. The robust, transient induction of the RNA-binding protein ZFP36 (also known as TTP and TIS11) (**Supplementary Fig. 4** online) suggests that it may function in degradation of short-lived, inducible mRNAs. ZFP36 binds to AU-rich elements (AREs), which are predominantly found within the 3′ UTR of unstable mRNAs[33], and promotes

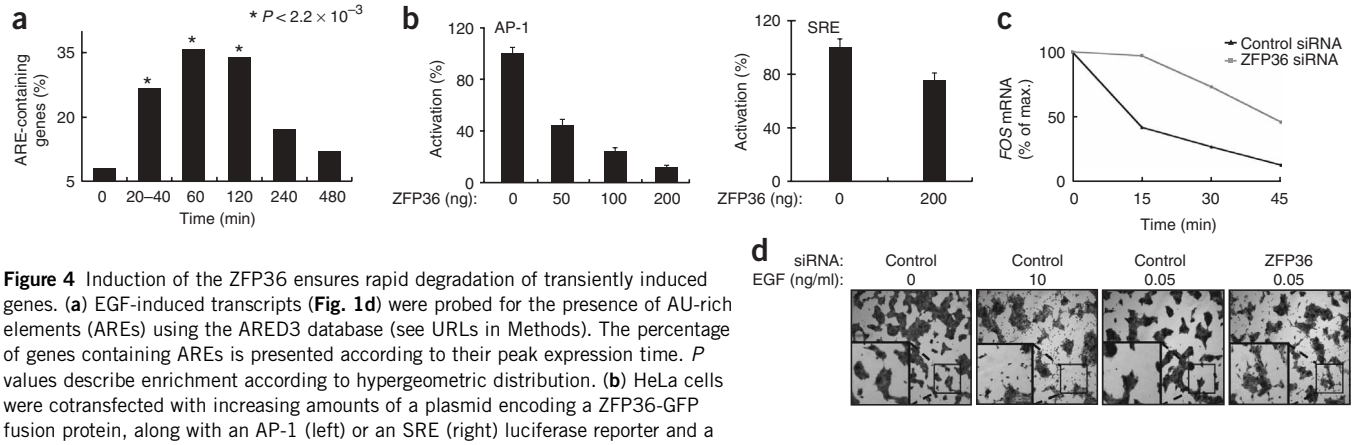

Figure 4 Induction of the ZFP36 ensures rapid degradation of transiently induced genes. (**a**) EGF-induced transcripts (**Fig. 1d**) were probed for the presence of AU-rich elements (AREs) using the ARED3 database (see URLs in Methods). The percentage of genes containing AREs is presented according to their peak expression time. *P* values describe enrichment according to hypergeometric distribution. (**b**) HeLa cells were cotransfected with increasing amounts of a plasmid encoding a ZFP36-GFP fusion protein, along with an AP-1 (left) or an SRE (right) luciferase reporter and a plasmid encoding constitutively active MEK. Relative luminescence signals were determined in triplicate 24 h later. Error bars in **b** and **c** represent s.d. (**c**) HeLa cells were transfected with ZFP36-specific siRNA (50 nM) oligonucleotides or with control oligonucleotides (50 nM). Twenty-four hours later, cells were serum-starved (12 h), stimulated with EGF (30 min) and exposed to actinomycin D for the indicated time intervals, followed by analysis of *FOS* mRNA by quantitative PCR. (**d**) MCF10A cells were transfected with control or ZFP36-specific siRNA oligonucleotides. Twenty-four hours later, the growth medium was changed to medium containing the indicated EGF concentrations. After an additional 24 h, cells were stained with crystal violet.

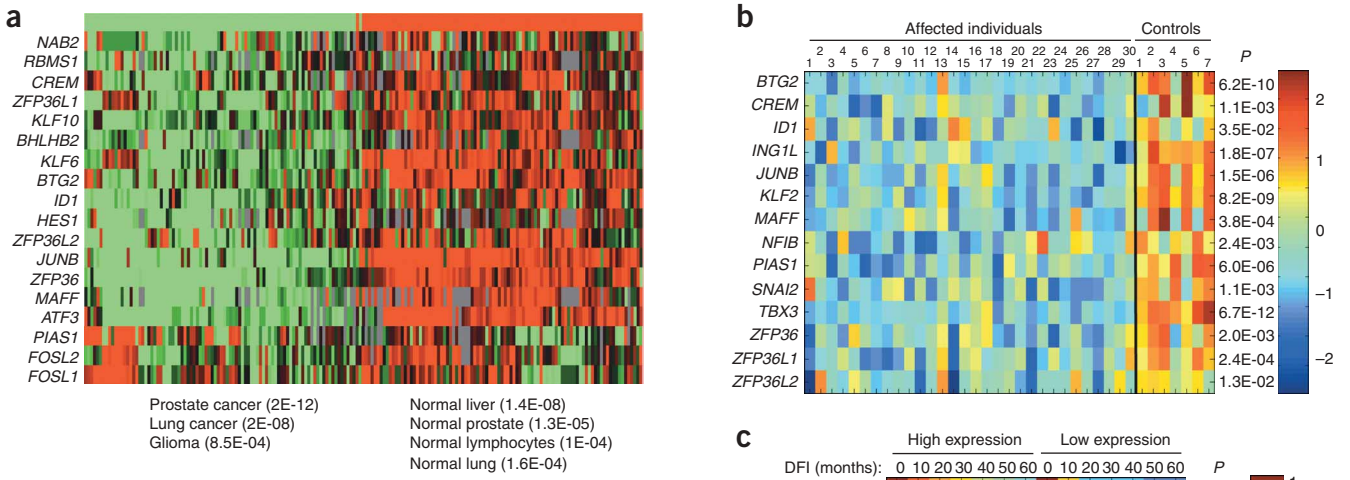

Figure 5 Transcription-repressor and RNA-binding DEGs are coordinately downregulated in multiple human tumors. (**a**) A subset of 25 DEGs was analyzed against a human cancer compendium[13] comprising 1,975 published microarrays across 22 tumor types, using the Genomica software package (see URLs in Methods). Shown are the arrays in which expression of the module changed significantly, where red indicates induction, and green, repression. Gray pixels represent missing values. Indicated below the matrix are tissues in which we observed significant repression (left) or induction (right) of the 25 DEGs. (**b**) The subset of 25 genes was analyzed against a data set derived from 30 ovarian tumors and 7 normal ovarian tissues. The expression matrix presents 14 genes in which we observed a significant difference between normal and malignant tissues. *t*-test *P* values are shown. (**c**) A group of 78 individuals with prostate cancer[50] was used to analyze the association between expression of transcription-repressor DEGs and survival time of affected individuals (different Kaplan-Meier survival analyses are shown). The color scale represents the fraction of individuals with no evidence of disease. DFI, disease-free interval. *P* values from Cox analysis are shown.

deadenylation and subsequent exosomal degradation of target mRNAs[34]. In order to characterize ZFP36 substrates (ARE-containing mRNAs), we grouped genes according to their peak expression time and determined, in each group, the frequency of ARE-containing transcripts (via the ARE Database search engine; see URL in Methods[35]). We found a significant preponderance of these motifs within the 3′ UTR of genes induced during the early waves of transcription (20–120 min; **Fig. 4a** and **Supplementary Table 1**). ZFP36 inhibited the transcriptional activity of AP-1 while not affecting transcription driven by the SRE. This result was expected, as AP-1 components are encoded by inducible ARE-containing mRNAs, and the SRE is activated by constitutively expressed phosphoregulated transcription factors[36] (**Fig. 4b** and **Supplementary Fig. 4**). Furthermore, small interfering RNA (siRNA) knockdown (**Supplementary Fig. 4**) demonstrated that ZFP36 is necessary for degradation of *FOS* mRNA (**Fig. 4c** and **Supplementary Fig. 4**). siRNA knockdown of ZFP36 in MCF10A cells, which dissociate from epithelial clusters and migrate in response to EGF stimulation[37], resulted in greatly enhanced sensitivity to EGF-driven cell motility, as measured by an increase in cell scattering (**Fig. 4d**) and migration (**Supplementary Fig. 4**). These results confirm the role of ZFP36 as an inducible attenuator of EGF signaling, promoting degradation of rapidly induced genes and thus restricting the responsiveness of the cell to stimulation. Observation of oncogenic mutations within the ARE of the *FOS* gene provides physiological evidence of the importance of this mode of regulation[38]. As we discuss below, in the context of a network, the activity of ZFP36 may promote the speed of IEG transcription by forming incoherent feed-forward loops[39]. Additional RNA-binding proteins of similar potential function were induced by EGF (**Supplementary Fig. 4**); for example, the late induction of heterogeneous nuclear ribonucleoprotein D (HNRPD, also known as Auf1)[40] is suggestive of a role in regulation of the expression of a subset of genes different from those regulated by ZFP36.

DEGs are potential tumor suppressors

Proteins that function as negative regulators of growth factor signaling have been found to act as tumor suppressors[41]. Exploring a large human cancer compendium[13] (comprising 1,975 published microarrays spanning 22 tumor types; see URLs for Genomica in Methods section), we examined the expression of genes from the DEG cluster of transcription repressors and RNA-binding proteins (**Supplementary Table 1**). We observed that a large proportion of these genes (18 of 25) were coordinately downregulated in multiple epithelial tumor types (**Fig. 5a**). Specifically addressing the expression of this group of genes in ovarian tumors (for which patient follow-up survival data were available), we found coordinate downregulation of a large subset of the transcription repressors (14 of 25) in tumor samples, consistent with observations of downregulation of *KLF2* and *KLF6* in ovarian tumors[25,42] (**Fig. 5b**). By contrast, expression of EGF-inducible ligands found in our data set (the output of forward signaling) was significantly upregulated in these tumors (**Supplementary Fig. 5** online). Furthermore, clinical follow-up showed that survival of affected individuals with low DEG level was significantly shorter than that of individuals with high levels of DEG. This held true for several other epithelial tumors (data not shown), including prostate cancer (**Fig. 5c**) as well as the ovarian cancer study presented here (**Supplementary Fig. 5**).

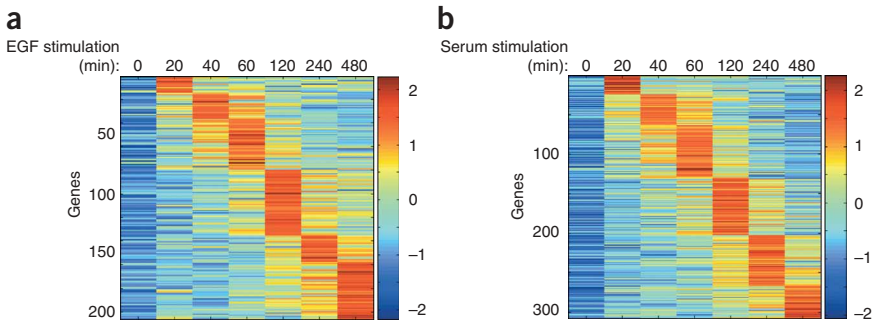

Figure 6 A common architecture underlies gene expression programs activated by stimulation of MCF10A cells with EGF or serum. (**a**,**b**) Subconfluent MCF10A cells, serum-starved for 24 h, were stimulated with EGF (20 ng/ml; **a**) or serum (**b**) over the course of 480 min, followed by analysis of RNA expression levels using Affymetrix Hu-133A oligonucleotide microarrays. Genes whose expression was induced to at least twice the baseline level are shown, sorted according to the time of peak expression.

components differed significantly (**Supplementary Table 1**). The transcriptional profiles of MCF10A cells treated with either EGF or serum shared 47% identity, whereas those of EGF-treated MCF10A and EGF-treated HeLa shared 36% identity.

As the three expression matrices share a common architecture, while differing in their components, we postulate that the particular combination of induced genes defines the identity of the active cellular pathways[43]. Focusing on the pattern of induction of dual-specificity phosphatases (DUSPs) across the three expression matrices, we addressed pathway specificity in the induction of feedback regulators. In HeLa cells, we observed activation of ERK, JNK and p38 MAPKs (**Fig. 1c**), mirrored by the transcriptional induction of a large number of DUSPs (**Fig. 7a**), which feed back to attenuate the activity of the MAPKs. Although some DUSPs are specific to ERK, others preferentially inactivate p38 and JNK[17]. In MCF10A cells, EGF stimulation resulted in specific activation of ERK, whereas serum specifically activated JNK (**Fig. 7b**). Consistent with pathway specificity in the induction of the DUSPs, EGF treatment of MCF10A cells resulted in predominant induction of ERK-specific *DUSP3*, *DUSP4*, *DUSP6* and *DUSP7*, whereas serum treatment resulted in predominant induction of the p38- and JNK-specific *DUSP1* and *DUSP10* (**Fig. 7c**). Moreover, inhibition of MEK in HeLa cells abolished the induction of the ERK-specific *DUSP6*, whereas treatment with a mixture of JNK and p38 inhibitors resulted in slightly elevated

Pathway-specific induction of feedback attenuation

To assess the implications of our observations beyond the model of EGF-stimulated HeLa cells, we turned to MCF10A, a normal human breast epithelial cell line. In these cells, EGF drove migration through the dominant circuit of ERK-EGR1 (see below, **Supplementary Fig. 6** online and data not shown), whereas serum factors ('serum') drive proliferation, predominantly through JNK-AP1 (data not shown). When examining the kinetic profile of EGF- and serum-induced gene expression in these cells, we found marked similarity in the pattern of gene expression induced by EGF in HeLa cells and the patterns induced by EGF and serum in MCF10A cells (**Fig. 6a**,**b**). Although the kinetics of induction of the gene clusters of IEGs, DEGs and cytokines (**Supplementary Fig. 6**) were conserved across the three transcriptional profiles, the identity of the

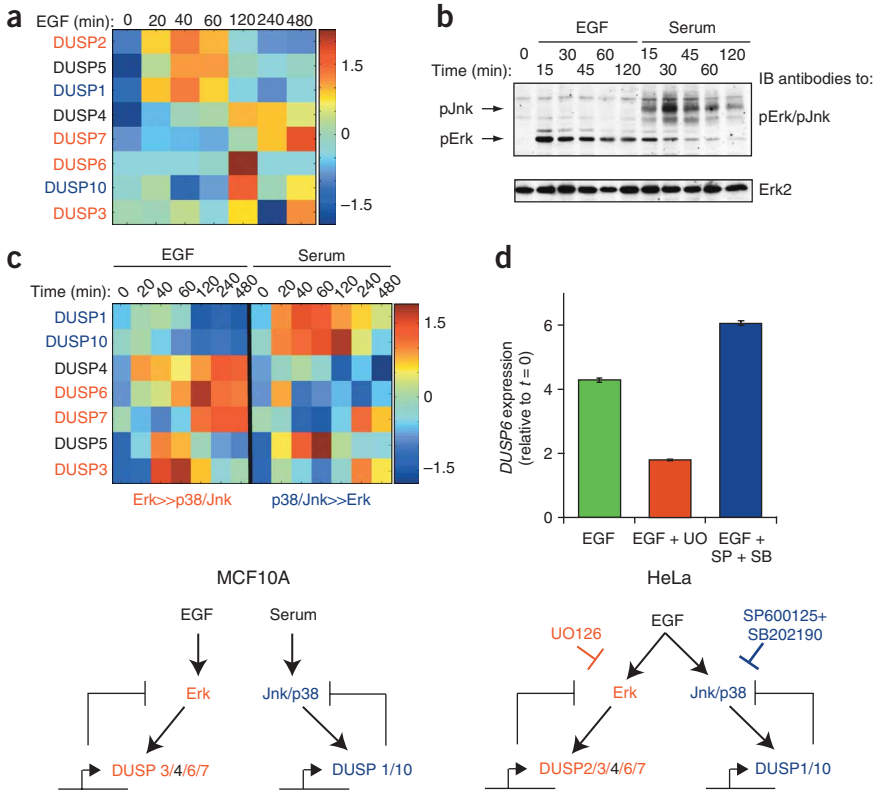

Figure 7 Pathway-specific induction of DUSPs. (**a**) Induction of DUSPs in EGF-stimulated HeLa cells (from HeLa expression data set). (**b**) Serum-starved MCF10A cells were stimulated with serum or EGF and were analyzed by immunoblotting (IB) for activation of the MAPKs ERK and JNK. ERK2 immunoblotting serves as a control. (**c**) Induction of DUSPs in EGF- or serum-stimulated MCF10A cells (from MCF10A expression data set). The chart underneath summarizes the differential activation of DUSPs: EGF-stimulated ERK leads to transcription of ERK-specific DUSPs (*DUSP3*, *DUSP4*, *DUSP6* and *DUSP7*) marked in red, whereas JNK and p38 stimulation by serum leads to induction of p38/JNK-specific DUSPs (*DUSP1* and *DUSP10*) marked in blue. (**d**) Quantitative PCR analysis of the expression of *DUSP6* after EGF stimulation of HeLa cells, in the presence of the MEK inhibitor U0126 (labeled UO) or the p38 and JNK inhibitors SB202190 (labeled SB) and SP600125 (labeled SP). Shown are mean ± s.d. for three replicates. The scheme underneath presents the differential activation of ERK and JNK/p38 by EGF, leading to transcription of the ERK-specific DUSPs and p38/JNK-specific DUSPs.

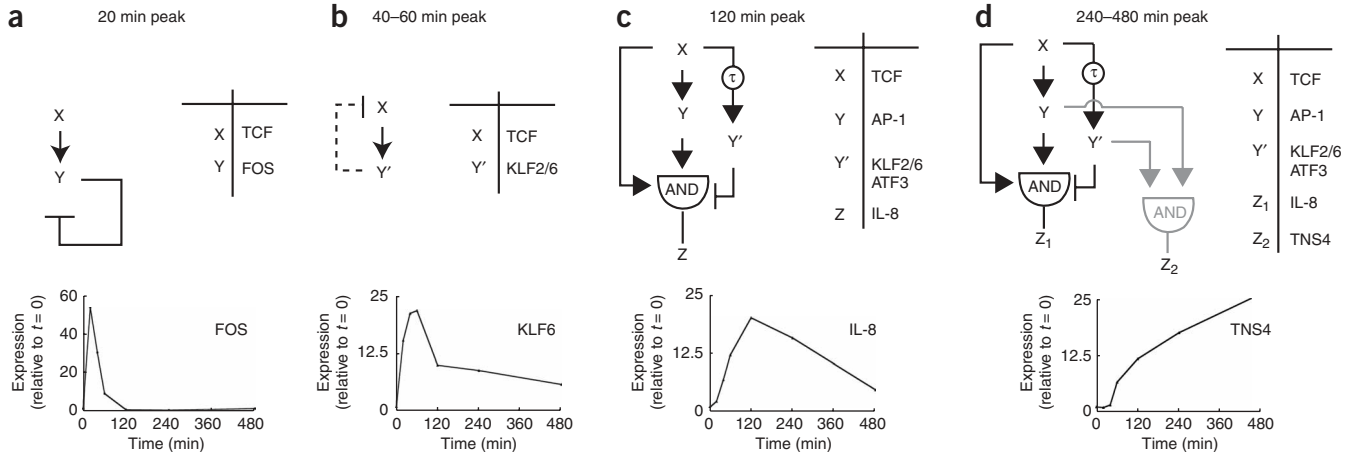

Figure 8 Potential network motifs used by the EGF-induced transcription program. (**a**) The early peak of *FOS* expression may be (at least in part) explained by a negative autoregulatory loop in which the newly synthesized FOS protein binds to its own promoter to attenuate transcription. (**b**) A composite negative feedback loop comprising a transcription activator (for example, TCF) whose activity is attenuated by its target gene (for example, a KLF family protein), resulting in transient activation of gene expression. (**c**) Two coupled feed-forward loops (FFLs) may generate expression profiles of late-induced cytokine genes like *IL8*. The 'coherent' FFL (potentially involving TCF (X) and AP-1 or EGR1 (Y)) generates a delay owing to a necessary accumulation of a transcriptional activator (such as AP-1 or EGR1), whereas the 'incoherent' FFL (potentially involving TCF (X) and KLF2, KLF6 or ATF3 (Y′)) shows an intrinsic delay (τ) in the induction of the transcriptional repressor Y′. This structure enables delayed induction of the target gene Z, which is shut down by the delayed activation of the repressor Y′. (**d**) Cascaded FFLs can generate a late wave of gene expression: Y′ participates as a repressor in an incoherent FFL (as in **c**), whereas it functions as an activator in a coherent FFL together with Y. This motif demonstrates a mechanism for slow accumulation of effectors, which may promote the transition to a new cellular state. All expression profiles are derived from the HeLa transcriptional data set.

expression of *DUSP6* (**Fig. 7d**). These observations are suggestive of a conserved architecture of signaling pathways whereby the output of the system depends on the precise dynamics of induction of forward- and backward-acting components. Furthermore, transcription-dependent attenuation of signaling involves induction of regulators specific to the inducing pathway.

Common motifs within the EGF-induced transcriptional network

Based on the kinetic data sets produced in this study and on previous observations relating to interactions between components of the network, we performed an initial analysis of the EGF network in terms of its functional architecture. In particular, we identified circuit elements called network motifs[2] that have been studied primarily in unicellular organisms. These are simple building blocks of robust networks, comprising a small number of components whose connectivities display a recurrent logic. Recognition of such elements may uncover the mechanisms underlying the kinetics of response to growth factor activation as well as the foundations of network robustness. Here we propose a set of simplified network motifs that model the activity of parts of the EGF-induced transcriptional program.

Examples of such motifs can be suggested for each epoch of gene expression (**Fig. 8**). Thus, *FOS*, the gene induced earliest by EGF, is regulated by a negative autoregulatory loop (**Fig. 8a** and ref. 29) that has been found to accelerate the response time within transcriptional networks[2]. The next wave of transcription (peaking at 40–60 min post-stimulation) undergoes 'superinduction' in the presence of cycloheximide, in common with the initial burst of IEG expression (data not shown). We propose that this wave may be regulated by a composite negative feedback loop in which the function of a 'forward-driving' transcription factor is attenuated by the protein product of its target gene(s) (**Fig. 8b**). This motif is found in diverse systems and organisms, where it generates a robust and transient induction[2].

The regulation of the next wave of gene expression (**Fig. 8c**; peaking at around 120 min after stimulation) may be explained as the output of two feed-forward loop motifs (FFLs)[2]. Each FFL consists of a transcription factor (Y) that activates a second transcription factor (Y′), both of which regulate a target gene, Z. One FFL is 'coherent', meaning that all arrows are of the same sign (in this case, positive). A coherent FFL generates a delay in activation because the transcriptional activator Y (for example, AP-1 or EGR1) must accumulate in order to drive induction of the output gene Z (exemplified by cytokines). The second type of FFL is an incoherent FFL (arrows are not of the same sign). In this FFL, Y′ is a slowly induced repressor that functions to attenuate the signaling in a delayed fashion. Thus, the output gene Z is induced with a delay by the coherent FFL, followed by delayed attenuation through the action of the incoherent FFL.

The last wave of gene expression in this study peaks at 240–480 min post-stimulation (**Fig. 8d**). A possible gene circuit that can correspond to these dynamics is a coherent FFL, based on two intermediate transcription factors (Y and Y′). In this proposed circuit, Y′ participates as a repressor in an incoherent FFL as well as an activator in a coherent FFL driving the expression of the late genes (for an example of opposite effects of a transcriptional regulator, see the effects of KLF2 on transcription driven by AP-1 or SP1 in **Supplementary Fig. 3**). Such a design has been found to generate a wave of late gene expression during *Bacillus subtilis* sporulation[44]. A similar mechanism has been demonstrated for the FOS gene product, where a 'master regulator' of transcription attenuates a preceding wave of transcription while positively promoting the subsequent wave of transcription[29]. Several additional network motifs tentatively identified in this system (**Supplementary Fig. 7** online) include a composite negative feedback loop involving transcription of DUSPs (to attenuate MAPK activation) as well as a self-attenuating FFL involving MAFF (**Supplementary Fig. 7**). However speculative, these motifs provide a useful platform to generate experimentally testable hypotheses.

DISCUSSION

In this study, we address the network architecture underlying the robust cellular response to growth factor stimulation, focusing on mechanisms of transcription-dependent feedback. Consistent with previous reports, we provide evidence that attenuation of MAPK signaling and IEG expression are dependent on *de novo* protein synthesis (**Fig. 1a**,**b** and refs. 7,8). In an attempt to identify the architecture of signaling pathway regulation, we have carried out a kinetic analysis of growth factor–driven transcription and have observed that distinct waves of transcription are induced after stimulation of cells.

The rapid induction of a limited set of 'forward-driving' transcription factors is followed by the delayed induction of a set of feedback regulators (**Figs. 1d**, **2** and **6**). In the case of the DUSPs, feedback regulators are induced by the pathways whose activity they attenuate (**Fig. 7**). A major constituent of this set are proteins that function in attenuation of gene expression through inhibition of transcriptional complexes, as well as by promoting degradation of the induced mRNAs (**Figs. 3** and **4**). Considering their role in attenuating growth factor signaling, we were not surprised to find that a significant proportion of the negative regulators are downregulated in multiple carcinomas (**Fig. 5a**,**b**). Furthermore, low expression of these genes correlates with poor prognosis (**Fig. 5c**). Association of the components described above into simple network motifs (**Fig. 8**) serves to clarify our understanding of how interactions between components of the network may bring about the observed system dynamics, and it serves as a basis for further experimentation.

The temporal organization uncovered in our study seems to be conserved across diverse mitogenic stimuli, as well as in different cell types. Indeed, similar patterns appear in distinct signaling cascades, such as those stimulated by EGF and serum in HeLa and MCF10A cells (**Figs. 1** and **6**), as well as tumor necrosis factor (TNF)-stimulated fibroblasts[45]. We propose that cells interpret information along the temporal axis: namely, that the timing of a signaling event encodes crucial information that may determine cellular decisions. Consequently, investigation of a given effector within a particular system should be most revealing in the appropriate temporal context.

The cellular response to stimulation involves the induction of a limited set of forward-signaling events, followed by a large cellular effort focused on signal attenuation in order to achieve tight control of the system. The final outcome is defined by multiple levels of signal integration. While one domain of integration is along the temporal axis, another may involve convergence of parallel pathways on various signaling nodes. In line with previous studies, temporal summation occurs also at the interface of signaling and transcription, such that the transcriptional activity of IEG protein products depends upon the duration of upstream kinase activity. This forms a feed-forward loop that functions as a persistence detector, enabling further signaling only in the presence of prolonged upstream kinase activation[46].

Notably, it has been demonstrated that prolonged versus brief activation of a signaling pathway may promote different cellular outcomes. This has been demonstrated for differentiation versus proliferation of PC12 cells[47] as well as for the distinct biological responses generated by TNF or lipopolysaccharide (LPS)[48]. These phenomena may be explained by observing the balance between forward-driving actions and feedback attenuation mechanisms. Short activation may occur through inactivation of the input, such as the rapid downregulation of the EGF receptor[49], favoring attenuation of the signal through the action of induced negative regulators. Conversely, the shift of the balance toward negative regulation may take longer when signaling is driven through receptors that do not undergo downregulation or inactivation, ultimately resulting in prolonged signaling. Another possible mechanism could be based on differing thresholds of transcriptional activation for positive effectors versus negative effectors. This might explain the difference between strong and transient induction of NFκB activity driven by TNF, in contrast to the persistent weak activation driven by LPS signaling[48].

In summary, we postulate the existence of a basic common architecture underlying the transcriptional response of a cell to growth factor stimulation. This structure evokes a dynamic temporal code of transcriptional complexes, resulting in transient waves of gene expression. These distinct clusters of genes encode proteins of similar function, ultimately defining the characteristics and outcome of cellular signaling. We conclude that the DEG cluster functions as a structured module defining the temporal domain of both signaling and transcription events in response to growth factor stimulation.

METHODS

Cell lines and RNA preparation. HeLa cells were grown in DMEM with 10% bovine serum supplemented with antibiotics, and MCF10A cells were grown in DME:F12 medium supplemented with antibiotics (10 μg/ml insulin, 0.1 μg/ml cholera toxin, 0.5 μg/ml hydrocortisone and heat-inactivated horse serum (5% vol/vol), defined as 'serum' in the text) and 10 ng/ml EGF. After the indicated treatments, cells (5×10^6 HeLa or 1×10^7 MCF10A cells per sample) were collected by scraping in PBS on ice. Cell pellets were then extracted and RNA was purified using Versagene's RNA isolation kit according to the manufacturer's protocol. The quality of RNA was verified by electrophoresis on a 1.5% agarose gel and by real-time PCR.

Real-time quantitative PCR and oligonucleotide microarray hybridization. cDNA was generated by the use of an Invitrogen SuperScriptII first-strand synthesis kit. Real-time PCR analysis was performed using SYBR Green I as a fluorescent dye, according to the manufacturer's guidelines. All experiments were carried out in triplicate, and results were normalized to beta-2 microglobulin RNA levels. Real-time PCR primers were designed using ProbeLibrary (see URLs below), and primer sequences are available in **Supplementary Methods** online. For oligonucleotide microarray hybridization, 10 μg RNA was labeled, fragmented and hybridized to an Affymetrix HG-U133A oligonucleotide array. After the arrays were scanned, the expression value for each gene was calculated using Affymetrix Microarray software 5.0 (MAS5). The average intensity difference values were normalized across the sample set. Probe sets that were absent in all samples according to Affymetrix flags were removed. All values lower than 50 were replaced by 50. Only probe sets that were upregulated by twofold or more were analyzed further in this study.

Luciferase reporter assays. STAT3, EGR1, SRE, NFκB, SP1 and AP-1 activities were measured after transfection of cells with plasmids (0.5 μg DNA) encoding the indicated response element fused to a luciferase reporter gene. Cells were subsequently split to 24-well plates and serum starved overnight before treatment as indicated with EGF (20 ng/ml) for 4 h. The luciferase reporter assay was performed using a Promega luciferase assay system. Light intensity was measured using a luminometer.

Expression vectors and siRNA. pEGFP vectors encoding GFP-KLF2 and GFP-MAFF were cloned from HeLa cDNA prepared from cells stimulated with EGF for 60 min. Deletions and point mutants were generated using the QuikChange mutagenesis kit (Stratagene) and PCR-based strategies. The following plasmids were gifts: ZFP36-GFP from P. Blackshear (National Institutes of Health), an IL8 reporter plasmid from M. Kracht (Medical School Hannover), EGR1 reporter plasmid from J. Milbrandt (Washington University School of Medicine) and a STAT3 reporter plasmid from A. Gertler (Hebrew University). siRNA oligonucleotide pools directed to *ZFP36* and control siRNA were obtained from Dharmacon. Oligofectamine and Lipofectamine (Invitrogen) were used for siRNA and plasmid transfections, respectively.

Lysate preparation and immunoblotting analysis. Cells were washed briefly with ice-cold saline and then scraped in solubilization buffer (50 mM HEPES (pH 7.5), 150 mM NaCl, 10% glycerol, 1% Triton X-100, 1 mM EDTA, 1 mM

EGTA, 10 mM NaF, 30 mM β-glycerol phosphate, 0.2 mM Na_3VO_4 and a protease inhibitor cocktail). For equal gel loading, protein concentrations were determined using the Bradford technique. After gel electrophoresis, proteins were electrophoretically transferred to a nitrocellulose membrane. Membranes were blocked in TBST buffer (0.02 M Tris-HCl (pH 7.5), 0.15 M NaCl and 0.05% Tween 20) containing 10% low-fat milk, blotted with a primary antibody for 1 h, washed with TBST and incubated for 30 min with a secondary antibody linked to horseradish peroxidase (HRP). Immunoreactive bands were detected using chemiluminescence.

Transwell cell migration assay. MCF10A cells (4×10^4 cells/well) were plated in the upper compartment of a 24-well Transwell tray (Corning) and allowed to adhere for 16 h at 37 °C in full medium lacking EGF. Thereafter, the medium in the lower compartment of the chamber was either refreshed or replaced with medium containing EGF, and cells were allowed to migrate through the intervening nitrocellulose membrane (8 μm pore size) for 16 h at 37 °C. The filter was removed and fixed for 15 min in PBS containing paraformaldehyde (3%), followed by cell permeabilization in Triton X-100 (0.05%, in PBS) and staining with methyl violet. Cells growing on the upper side of the filter were scraped using a cotton swab, and cells growing on the bottom side of the filter were photographed and counted.

Survival analysis. The outcome correlation analysis reports the *P* value of the COX analysis. The cutoff of the high and low groups was optimized to achieve the most significant *P* value with at least 20% patients at each group. A color-code display of fraction of survival or disease-free interval replaces the traditional Kaplan-Meier survival curves. In this display (**Fig. 5c** and **Supplementary Fig. 5**), every row is a gene, and every column is a time period in the high-expression group or the low-expression group. A color code gives the fraction of surviving or disease-free individuals in the group with high or low expression of this gene at a given time point. For additional information see **Supplementary Methods**.

Accession codes. The complete microarray data sets are available from the Gene Expression Omnibus (GSE6786).

URLs. Gene Ontology database: http://www.geneontology.org; Human Protein Reference Database: http://www.hprd.org; ARED3 database: http://rc.kfshrc.edu.sa/ared3/Search_Main.aspx; Genomica: http://genomica.weizmann.ac.il; ProbeLibrary: http://www.probelibrary.com.

Note: Supplementary information is available on the Nature Genetics website.

ACKNOWLEDGMENTS

We thank P. Blackshear, W. Lai, M. Kracht, J. Milbrandt, S. Friedman and G. Narla for reagents. We thank P. Luu, R. Malenka and N. Citri for instructive comments on the manuscript. We thank W.L. Gerald for providing us with the prostate cancer data set. The following plasmids were gifts: ZFP36-GFP from P. Blackshear (National Institutes of Health), an IL8 reporter plasmid from M. Kracht (Medical School Hannover), EGR1 reporter plasmid from J. Milbrandt (Washington University School of Medicine) and a STAT3 reporter plasmid from A. Gertler (Hebrew University). Our laboratory is supported by research grants from Minerva, the Israel Cancer Research Fund, the German Israel Foundation, the Prostate Cancer Foundation, the European Commission and the National Cancer Institute (grants CA72981, CA102537, CA65930, CA64602 and CA099031). Y.Y. is the incumbent of the Harold and Zelda Goldenberg Professorial Chair, and E.D. is the incumbent of the Henry J. Leir Professorial Chair. A.C. acknowledges support of the Human Frontier Science Program. E.D. was supported in part by the Ridgefield Foundation, the Israel Science Fund and the European Commission (EC FP6). Requests for materials should be addressed to Y.Y. (yosef.yarden@weizmann.ac.il).

COMPETING INTERESTS STATEMENT

The authors declare no competing financial interests.

Published online at http://www.nature.com/naturegenetics
Reprints and permissions information is available online at http://npg.nature.com/reprintsandpermissions

1. Freeman, M. Feedback control of intercellular signalling in development. *Nature* **408**, 313–319 (2000).
2. Alon, U. *An Introduction to Systems Biology: Design Principles of Biological Circuits* (CRC Press, Boca Raton, Florida, 2006).
3. Kholodenko, B.N. Cell-signalling dynamics in time and space. *Nat. Rev. Mol. Cell Biol.* **7**, 165–176 (2006).
4. Citri, A. & Yarden, Y. EGF-ERBB signalling: towards the systems level. *Nat. Rev. Mol. Cell Biol.* **7**, 505–516 (2006).
5. Hynes, N.E. & Lane, H.A. ERBB receptors and cancer: the complexity of targeted inhibitors. *Nat. Rev. Cancer* **5**, 341–354 (2005).
6. Shaulian, E. & Karin, M. AP-1 as a regulator of cell life and death. *Nat. Cell Biol.* **4**, E131–E136 (2002).
7. Sun, H., Charles, C.H., Lau, L.F. & Tonks, N.K. MKP-1 (3CH134), an immediate early gene product, is a dual specificity phosphatase that dephosphorylates MAP kinase in vivo. *Cell* **75**, 487–493 (1993).
8. Lau, L.F. & Nathans, D. Expression of a set of growth-related immediate early genes in BALB/c 3T3 cells: coordinate regulation with c-fos or c-myc. *Proc. Natl. Acad. Sci. USA* **84**, 1182–1186 (1987).
9. Sheehan, K.M. *et al.* Use of reverse phase protein microarrays and reference standard development for molecular network analysis of metastatic ovarian carcinoma. *Mol. Cell. Proteomics* **4**, 346–355 (2005).
10. Casci, T. & Freeman, M. Control of EGF receptor signalling: lessons from fruitflies. *Cancer Metastasis Rev.* **18**, 181–201 (1999).
11. Jones, S.M. & Kazlauskas, A. Growth-factor-dependent mitogenesis requires two distinct phases of signalling. *Nat. Cell Biol.* **3**, 165–172 (2001).
12. Klein, O.D. *et al.* Sprouty genes control diastema tooth development via bidirectional antagonism of epithelial-mesenchymal FGF signaling. *Dev. Cell* **11**, 181–190 (2006).
13. Segal, E., Friedman, N., Koller, D. & Regev, A. A module map showing conditional activity of expression modules in cancer. *Nat. Genet.* **36**, 1090–1098 (2004).
14. Iyer, V.R. *et al.* The transcriptional program in the response of human fibroblasts to serum. *Science* **283**, 83–87 (1999).
15. Kalir, S. *et al.* Ordering genes in a flagella pathway by analysis of expression kinetics from living bacteria. *Science* **292**, 2080–2083 (2001).
16. Zhang, W. *et al.* The functional landscape of mouse gene expression. *J. Biol.* **3**, 21 (2004).
17. Farooq, A. & Zhou, M.M. Structure and regulation of MAPK phosphatases. *Cell. Signal.* **16**, 769–779 (2004).
18. Qu, Z. *et al.* The transcriptional corepressor NAB2 inhibits NGF-induced differentiation of PC12 cells. *J. Cell Biol.* **142**, 1075–1082 (1998).
19. Hoffmann, E. *et al.* MEK1-dependent delayed expression of Fos-related antigen-1 counteracts c-Fos and p65 NF-kappaB-mediated interleukin-8 transcription in response to cytokines or growth factors. *J. Biol. Chem.* **280**, 9706–9718 (2005).
20. Szabowski, A. *et al.* c-Jun and JunB antagonistically control cytokine-regulated mesenchymal-epidermal interaction in skin. *Cell* **103**, 745–755 (2000).
21. Yates, P.R., Atherton, G.T., Deed, R.W., Norton, J.D. & Sharrocks, A.D. Id helix-loop-helix proteins inhibit nucleoprotein complex formation by the TCF ETS-domain transcription factors. *EMBO J.* **18**, 968–976 (1999).
22. Gilchrist, M. *et al.* Systems biology approaches identify ATF3 as a negative regulator of Toll-like receptor 4. *Nature* **441**, 173–178 (2006).
23. Fu, S., Bottoli, I., Goller, M. & Vogt, P.K. Heparin-binding epidermal growth factor-like growth factor, a v-Jun target gene, induces oncogenic transformation. *Proc. Natl. Acad. Sci. USA* **96**, 5716–5721 (1999).
24. Barton, K. *et al.* Defective thymocyte proliferation and IL-2 production in transgenic mice expressing a dominant-negative form of CREB. *Nature* **379**, 81–85 (1996).
25. Narla, G. *et al.* KLF6, a candidate tumor suppressor gene mutated in prostate cancer. *Science* **294**, 2563–2566 (2001).
26. Motohashi, H., Katsuoka, F., Shavit, J.A., Engel, J.D. & Yamamoto, M. Positive or negative MARE-dependent transcriptional regulation is determined by the abundance of small Maf proteins. *Cell* **103**, 865–875 (2000).
27. Wisdom, R. & Verma, I.M. Proto-oncogene FosB: the amino terminus encodes a regulatory function required for transformation. *Mol. Cell. Biol.* **13**, 2635–2643 (1993).
28. Das, H. *et al.* Kruppel-like factor 2 (KLF2) regulates proinflammatory activation of monocytes. *Proc. Natl. Acad. Sci. USA* **103**, 6653–6658 (2006).
29. Sassone-Corsi, P., Sisson, J.C. & Verma, I.M. Transcriptional autoregulation of the proto-oncogene fos. *Nature* **334**, 314–319 (1988).
30. Sevetson, B.R., Svaren, J. & Milbrandt, J. A novel activation function for NAB proteins in EGR-dependent transcription of the luteinizing hormone beta gene. *J. Biol. Chem.* **275**, 9749–9757 (2000).
31. Kaszubska, W. *et al.* Cyclic AMP-independent ATF family members interact with NF-kappa B and function in the activation of the E-selectin promoter in response to cytokines. *Mol. Cell. Biol.* **13**, 7180–7190 (1993).
32. Claret, F.X., Hibi, M., Dhut, S., Toda, T. & Karin, M. A new group of conserved coactivators that increase the specificity of AP-1 transcription factors. *Nature* **383**, 453–457 (1996).
33. Carballo, E., Lai, W.S. & Blackshear, P.J. Feedback inhibition of macrophage tumor necrosis factor-alpha production by tristetraprolin. *Science* **281**, 1001–1005 (1998).
34. Chen, C.Y. *et al.* AU binding proteins recruit the exosome to degrade ARE-containing mRNAs. *Cell* **107**, 451–464 (2001).
35. Bakheet, T., Williams, B.R. & Khabar, K.S. ARED 3.0: the large and diverse AU-rich transcriptome. *Nucleic Acids Res.* **34**, D111–D114 (2006).
36. Sharrocks, A.D. The ETS-domain transcription factor family. *Nat. Rev. Mol. Cell Biol.* **2**, 827–837 (2001).
37. Irie, H.Y. *et al.* Distinct roles of Akt1 and Akt2 in regulating cell migration and epithelial-mesenchymal transition. *J. Cell Biol.* **171**, 1023–1034 (2005).

38. Meijlink, F., Curran, T., Miller, A.D. & Verma, I.M. Removal of a 67-base-pair sequence in the noncoding region of protooncogene fos converts it to a transforming gene. *Proc. Natl. Acad. Sci. USA* **82**, 4987–4991 (1985).
39. Mangan, S., Itzkovitz, S., Zaslaver, A. & Alon, U. The incoherent feed-forward loop accelerates the response-time of the gal system of *Escherichia coli*. *J. Mol. Biol.* **356**, 1073–1081 (2006).
40. Lu, J.Y., Sadri, N. & Schneider, R.J. Endotoxic shock in AUF1 knockout mice mediated by failure to degrade proinflammatory cytokine mRNAs. *Genes Dev.* **20**, 3174–3184 (2006).
41. Trotman, L.C. *et al.* Identification of a tumour suppressor network opposing nuclear Akt function. *Nature* **441**, 523–527 (2006).
42. Wang, F. *et al.* Transcriptional repression of WEE1 by Kruppel-like factor 2 is involved in DNA damage-induced apoptosis. *Oncogene* **24**, 3875–3885 (2005).
43. Bild, A.H. *et al.* Oncogenic pathway signatures in human cancers as a guide to targeted therapies. *Nature* **439**, 353–357 (2006).
44. Eichenberger, P. *et al.* The program of gene transcription for a single differentiating cell type during sporulation in *Bacillus subtilis*. *PLoS Biol.* **2**, e328 (2004).
45. Hoffmann, A., Leung, T.H. & Baltimore, D. Genetic analysis of NF-kappaB/Rel transcription factors defines functional specificities. *EMBO J.* **22**, 5530–5539 (2003).
46. Murphy, L.O., Smith, S., Chen, R.H., Fingar, D.C. & Blenis, J. Molecular interpretation of ERK signal duration by immediate early gene products. *Nat. Cell Biol.* **4**, 556–564 (2002).
47. Marshall, C.J. Specificity of receptor tyrosine kinase signaling: transient versus sustained extracellular signal-regulated kinase activation. *Cell* **80**, 179–185 (1995).
48. Werner, S.L., Barken, D. & Hoffmann, A. Stimulus specificity of gene expression programs determined by temporal control of IKK activity. *Science* **309**, 1857–1861 (2005).
49. Levkowitz, G. *et al.* Ubiquitin ligase activity and tyrosine phosphorylation underlie suppression of growth factor signaling by c-Cbl/Sli-1. *Mol. Cell* **4**, 1029–1040 (1999).
50. Stephenson, A.J. *et al.* Integration of gene expression profiling and clinical variables to predict prostate carcinoma recurrence after radical prostatectomy. *Cancer* **104**, 290–298 (2005).